Analytical Methods

Accepted Manuscript

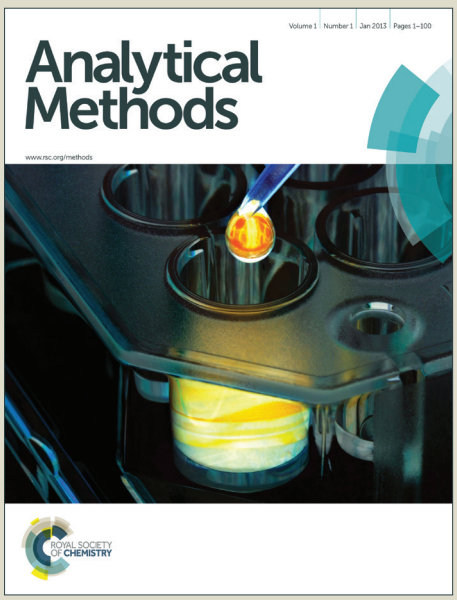

ROYAL SOCIETY OF CHEMISTRY

www.rsc.org/methods

A novel platform for detection of protooncogene based on Au nanoclusters enhanced fluorescence

Kang Mao[a], Yizhen Liu[a,b], Huaming Xiao[a], Yinran Chen[a], Zitong Wu[a], Xiaodong Zhou*[a], Aiguo Shen[a] and Jiming Hu[a]

a Key Laboratory of Analytical Chemistry for Biology and Medicine (Ministry of Education), College of Chemistry and Molecular Sciences, Wuhan University, Wuhan, 430072, China.

b College of Chemistry and Chemical Engineering, Shenzhen University, Shenzhen 518060, Guangdong, China

**Corresponding author. Tel.: +86 027 68752439-8116*

E-mail: zhouxd@whu.edu.cn

ABSTRACT

For the first time, gold nanoclusters was found to exhibit high fluorescence enhancement ability based on metal-enhanced fluorescence (MEF) effect, which can effectively enhance the fluorescence of fluorescein isothiocyanate (FITC). By means of this phenomenon, Au nanoclusters have been successfully used in the construction of a fluorescence-enhanced sensing platform for the detection of protooncogene.

Keywords: Au nanoclusters (AuNCs); fluorescein isothiocyanate (FITC); fluorescence enhancement; protooncogene

1. Introduction

Fluorescence-based detection technology, in combination with nanotechnology, has been widely used in biological fields.[1-4] A number of fluorescent nanomaterials, including quantum dots,[1] up conversion nanoparticles [2] and dye-doped nanoparticles,[3] are of considerable interest as sensors and indicators for biological detections due to their high fluorescence intensity, stability, and easy modification. To further increase fluorescence intensities of nanomaterial-based probes, metal nanostructures and dye molecules have been combined to fabricate metal-dye nanocomposites. It has been proven that fluorescence can be enhanced by several folds when the metal nanostructures and dye molecules are kept within a certain distance, but weakened or quenched othewise.[5-7] Such a fluorescence enhancement phenomenon is well-known as the metal-enhanced fluorescence (MEF) effect. The mechanisms of MEF have been extensively studied and several pathways of metal enhancement have been proposed.[8-14] First of all, the occurrence of surface plasmon resonance (SPR) leads to a strongly enhanced absorption of the incident light.[14-16] In fact, surface plasmon resonance has been widely used in explaining some interesting phenomenon such as enhancement of the photoluminescence,[15,16] plasmon-controlled Förster Resonance Energy Transfer (FRET),[17] enhanced energy transfer between quantum dots (QDs) and nanoparticles,[18-20] metal-enhanced surface plasmon-coupled phosphorescence,[21] surface-enhanced Raman scattering (SERS)[22] and plasmon-enhanced surface catalysis.[23] Considering the fluorescence enhancement, when the surface plasmon resonance band of a metal nanostructure overlaps the excitation of the fluorophore, the energy is transferred from the metal to the fluorophores so that the possibility of excitation of the dye molecules is increased. Secondly, the metal nanostructure can change the radiative deactivation rate of the fluorophores. Thus, the fluorescence lifetime and the quantum yield are changed.[24] Thirdly, the scattering of the metallic nanostructures affects the coupling efficiency of the fluorescence emission to the far field.[25, 26] By regulating the plasmon resonance band to the fluorophore emission wavelength, a fluorescence enhancement can be obtained. Also, the rapid development of nanotechnology has produced various new types of metallic nanostructures, which generates a number of new effects of metallic nanomaterials on dye molecular properties, such as the dimensional effects of metallic nanostructures on fluorescence intensity.[27]

The fuorescence of metal nanoclusters has drawn continuous research interest in the fields of chemistry, biology and materials.[4, 28-32] There has been a great deal of research work on the fluorescence of metal nanoclusters, especially gold and silver.[29, 31, 33, 34] Owing to their ultrasmall size, biocompatibility and highly fluorescent properties, fluorescent gold nanoclusters (AuNCs) have become an attractive field of study. Up to now, the applications of fluorescent AuNCs in analysis are mainly based on the fluorescence quenching effect [33, 35] of AuNCs through the interaction between gold and the limited analytes like Fe^{3+},[36] Hg^{2+},[37, 38] Cu^{2+} [39, 40] and cysteine.[41] Also, AuNCs is as novel optical probes for in vitro and in vivo fluorescence imaging,[29, 42] As we know, the fluorescence of AuNCs correlates not only with the metal quantization effect but also with the surface ligands or scaffolds.[43] How to rationally design fluorescent AuNCs with functional ligands or scaffolds to give them broad applications remains to be explored.

According to the mechanisms of metal enhancement proposed above, for the first time, we report a simple and homogeneous assay format for protooncogene by using BSA-protected gold nanoclusters-based enhanced fluorogenic nanoprobes. Except high selectivity and sensitivity，this mix-and-detect assay format is simple. Importantly, the assay is homogeneous because it occurs exclusively in the liquid phase, which makes it easy to automate or suitable for in situ detection.

2. Materials and methods

2.1. Materials

All oligonucleotides (P1: 5′-FITC-CGCTCCAGAGGCAGTAACCAGAGCGTTTTTTTTTT-$(CH_2)_6$-SH-3′; T1: 5′-TGGTTACCGCCTCTG-3′; ssDNA1: 5′-TGGTTACTGCCTCTG-3′; ssDNA2: 5′-CCAACCTGTCTTTCCTACG-3′; ssDNA3: 5′-AACCTGTCTTTCCTACG-3′; ssDNA4: 5′-CCTGTCTTTCCTACG -3′) were purchased from Sangon Biotech (Shanghai, China) Co. Ltd. and purified by HPLC. The deionized water was purified using a Millipore filtration system (18.2 MΩ resistivity) and used in all experiments. All the experiments were carried out in phosphate buffer saline (PBS) buffer (0.1 mM PBS, 0.1 M NaCl, pH 8.00).

2.2. Instrumentation

The size distribution and structure of the AuNCs were probed by high-resolution transmission electron microscopy (HRTEM) using a JEM-2100 (HR) operated at an acceleration voltage of 200KV. Fluorescence spectrometer (F-4600, Hitachi Co. Ltd., Japan) with a Xenon lamp excitation source was employed to record fluorescence spectra. The excitation was set at 490 nm and the emission was monitored at 520 nm.

2.3. Synthesis of red fluorescent AuNCs

According to literature,[44] all glassware was washed with aqua regia ($HCl:HNO_3$ volume ratio=3:1) and rinsed with ethanol and ultrapure water (Caution: Aqua Regia is a very corrosive oxidizing agent, which should be handled with great care). In atypical experiment, aqueous $HAuCl_4$ solution (5 mL, 10 mM, 37°C) was added to BSA solution (5 mL, 50 mg/mL, 37 °C) under vigorous stirring. NaOH solution (0.5 mL, 1 M) was introduced 2 min later and the reaction was allowed to proceed under vigorous stirring at 37°C for 12 h. The obtained suspension was centrifuged and suspended with water before further characterizations and applications.

2.4. Fluorescence spectra measurements

The fluorescent probe P1 (10 nM) was hybridized with different amounts of T1 for 30 min in a PBS buffer solution of 195 μl, prior to the addition of the AuNCs solution (5 μl). The final

concentration of T1 ranged from 0 to 60 nM. For kinetic study of fluorescence enhancement, fluorescence spectra were recorded immediately after addition of AuNCs into P1 solution. For DNA assays, the fluorescence measurements were performed after incubated with AuNCs for 30 min. Fluorescence spectrometer (F-4600, Hitachi Co. Ltd., Japan) with a Xenon lamp excitation source was employed to record fluorescence spectra. The excitation was set at 490 nm and the emission was monitored at 520 nm.

3. Results and discussion

3.1. Fluorescence enhancement between FITC-tagged ssDNA and Au nanoclusters

The proposed mix-and-detect strategy is depicted in Scheme 1. In our process, two important factors, the adhension layer and the distance,[45,47] between the fluorophores and AuNCs, which exert great influence on fluorescence enhancement have been examined. The crucial role of the adhesion layer in plasmonic fluorescence enhancement has been reported by Heykel Aouani's group.[46] In Rizia Bardhan's report,[47] Au nanoshells (NSs) and Au nanorods wrapped in human serum albumin (HSA) were used as substrates, which more effectively enhanced the fluorescence compared with pure fluorophores. Like HSA and bovine serum albumin (BSA) were widely used in most studies as stabilizer and reducer to form fluorescent AuNCs. Thus, BSA was chosen in our study as the adhension layer to protect AuNCs.[44] As to the influence of the distance between the fluorophores and AuNCs on fluorescence enhancement, the ideal distance for maximum enhancement reported was 5-11 nm.[47] In our study, DNA techniques were applied to adjust the distance between AuNCs and fluorophores (FITC).

In our strategy, quantitative readout of the target DNA can be realized through the following principle and process. Based on the mechanisms of metal enhancement about surface plasmon resonance enhanced energy transfer, BSA-protected Au nanoclusters can be used as the donor [48] and FITC is the acceptor. When the distance between AuNCs and FITC controlled by DNA is perfect, the fluorescence of FITC is enhanced strongly. We expect that AuNCs can adsorb dye-labeled single-stranded DNA (ssDNA, the hairpin structure) probe via the Au-S force between SH and the AuNCs and then enhance the fluorescence of the dye.[41] In contrast, when a ssDNA probe is hybridized with its complementary target DNA, because the nucleobases are buried between the densely negatively charged helical phosphate backbones, the dye-labeled probe is away from the surface of AuNCs, resulting in getting rid of the fluorescence enhancement of the probe. As a result, the fluorescence of the probe is expected to provide a quantitative readout of the target DNA. In this work, protooncogene acts as the target DNA.

In our experiments, the AuNCs was synthesized through the reduction of chloroauric acid with bovine serum albumin (BSA) at physiological temperature using recently developed method[44] (see in Figure S1). The fluorescence enhancement ability of AuNCs toward the FITC-labeled ssDNA was evaluated via measurements upon mixing the fluorescent probe (FITC) and the prepared AuNCs. The FITC-labeled ssDNA probe (P1) used here is for a protooncogene aptamer. In the presence of AuNCs, the fluorescence of P1 was obviously enhanced (see the curve of P1+AuNCs in Figure 1). The enhancement kinetics was very fast, with up to more than 2 times fluorescence intensity obtained within 4 min after P1 was mixed with the AuNCs solution (see the curve of P1+AuNCs in the inset of Figure 1), which suggested that the interaction between FITC and AuNCs is quite strong and the AuNCs possesses a high fluorescence enhancement ability. In

addition, temperature from 20°C to 35°C has little effect on fluorescence enhancement of FITC (see in Figure 2).

Considering that the fluorescence stability is highly pH dependent, we studied the effects of pH on the fluorescence enhancement. According to the Figure 3, enormous changes of fluorescence of FITC with different pH from 5.5 to 10.0 have happened. According to previous reports, this is caused by the alternation of fluorescein structure between lactone and open loop tautomerism with different pH. Under alkaline conditions, lactone is the main form and two hydroxide radicals will have a certain degree of take off (with weak fluorescence). Under acidic conditions, the main form is open loop (neutral molecules or proton, and weak fluorescence). Thus, when the pH value increases, the fluorescence of FITC gets enhanced. Taking into account the effect of different pH on fluorescence intensity (above) and Hoogsteen base pairing, 8 is the best suitable pH value.

When the distance between FITC-labeled ssDNA and AuNCs is too wide, the fluorescence would decerease. It is known that the fluorescence can be significantly enhanced when P1 is mixed with AuNCs. However, when P1 was hybridized with an equal amount of the complementary target DNA T1 to form dsDNA, the P1/T1 duplex, the fluorescence largely decreased (see the curve of P1/T1+AuNCs in Figure 1). This was because the distance between FITC-labeled ssDNA and AuNCs was widened when T1 was added. The result confirmed the influence of the distance between FITC and AuNCs on the fluorescence enhancement intensity.

On the basis of the aforementioned findings, by adjusting the distance between FITC and AuNCs and keeping the pH value at the ideal level, a sensing platform for quantitative DNA assay can be built using AuNCs with high fluorescence enhancement ability.

3.2. Assay for protooncogene in aqueous buffer

In the experiment to determine the linear range of our DNA sensor, 10 nM of P1 was hybridized with T1 at various concentrations at room temperature for 30 min, and then the mixture was incubated with an aliquot of AuNCs solution. As the concentration of T1 increased, the percentage of P1 hybridized with T1 to form duplex also increased. As a result, the enhanced fluorescence of P1 decreased (Figure 4a). Note that the fluorescence could still decrease when the concentration of T1 exceeded that of P1. That might result from the absorption of T1 by AuNCs, which stopped part of T1 from being formed into the P1/T1 duplex. On the basis of the Figure 4b, this DNA sensor shows a linear range between 8 and 40 nM (R^2=0.992), with a detection limit of 4 nM (3 times the standard deviation rule), which is simple and homogeneous.

3.3. Selectivity assays

In addition, control experiments were conducted to confirm that the decreased fluorescence was due to the specific DNA structural switching. Four other types of mismatch ssDNA were systemically studied with the same assay protocol. However, none of the four analogues could induce the distinct fluorescence decrease, even at a very high concentration (10 uM), as compared to the P1 sample (Figure 5). This result has proven that the described mix-and-detect assay is highly selective toward protooncogene.

4. Conclusion

In conclusion, for the first time, we have revealed that when kept within a certain distance with FITC and when the pH value is suitable, AuNCs possesses high fluorescence enhancement

efficiency. Inspired by these findings, we employed AuNCs in the construction of a sensing platform for the quantitative detection of specific DNA. This mix-and-detect assay format is simple. Importantly, the assay is homogeneous because it occurs exclusively in the liquid phase, which makes it easy to automate or suitable for in situ detection. In addition, AuNCs can be readily synthesized on a large scale and used as efficient fluorescence enhancement nanomaterials without further processing. What's worth mentioning is that aptamers in vitro selected nucleic acid molecules with high specificity and affinity toward a wide spectrum of targets[49] are widely recognized as promising candidates for biosensing due to their intrinsic advantages.[50, 51] Besides the DNA hybridization, specific aptamer-target recognition can induce dramatic structural switching of the DNA probe.[52] Combined with the use of assorted aptamers, the ability of AuNCs to discriminate specific DNA could offer a new approach to detect a broad range of analytes. What's not neglectable is the high fluorescence of the AuNCs itself which allows it to be widely used in the emerging multiplex fluorescence imaging in biological applications in the near future. With these remarkable advantages, we believe this work provides opportunities to develop simple, rapid, and low-cost nanoprobes for molecular diagnostics.

Acknowledgments

We gratefully acknowledge the support from the Natural Science Foundation of China (NSFC) (No. 20927003, 90913013, 41273093 and 21175101), the National Major Scientific Instruments and Device Development Project (2012YQ16000701) and the Foundatio of China Geological Survey (Grant No. 12120113015200).

References

1. J. H. Warner, A. Hoshino, K. Yamamoto and R. Tilley, *Angew. Chem. Int. Ed.*, 2005, **117**, 4626-4630.
2. S. F. Lim, R. Riehn, C.-K. Tung, W. S. Ryu, R. Zhuo, J. Dalland and R. H. Austin, *Nanotechnology*, 2009, **20**, 405701.
3. S.-Y. Liu, L. Huang, J.-F. Li, C. Wang, Q. Li, H.-X. Xu, H.-L. Guo, Z.-M. Meng, Z. Shi and Z.-Y. Li, *J. Phys. Chem. C*, 2013, **117**, 10636-10642.
4. Y. Bao, C. Zhong, D. M. Vu, J. P. Temirov, R. B. Dyer and J. S. Martinez, *J. Phys. Chem. C*, 2007, **111**, 12194-12198.
5. B. Yang, N. Lu, D. Qi, R. Ma, Q. Wu, J. Hao, X. Liu, Y. Mu, V. Reboud and N. Kehagias, *Small*, 2010, **6**, 1038-1043.
6. K. Aslan, M. Wu, J. R. Lakowicz and C. D. Geddes, *J. Am. Chem. Soc.*, 2007, **129**, 1524-1525.
7. J. Zhang and J. R. Lakowicz, *Opt. Express*, 2007, **15**, 2598-2606.
8. P. K. Jain, W. Huang and M. A. El-Sayed, *Nano Lett.*, 2007, **7**, 2080-2088.
9. P. K. Jain and M. A. El-Sayed, *J. Phys. Chem. C*, 2008, **112**, 4954-4960.
10. W. Huang, W. Qian, P. K. Jain and M. A. El-Sayed, *Nano Lett.*, 2007, **7**, 3227-3234.
11. M. Mahmoud and M. El-Sayed, *J. Phys. Chem. C*, 2007, **111**, 17180-17183.
12. P. K. Jain, K. S. Lee, I. H. El-Sayed and M. A. El-Sayed, *J. Phys. Chem. B*, 2006, **110**, 7238-7248.
13. P. K. Jain, X. Huang, I. H. El-Sayed and M. A. El-Sayed, *Plasmonics*, 2007, **2**, 107-118.
14. Q.C. Sun, H. Mundoor, J. C. Ribot, V. Singh, I. I. Smalyukh and P. Nagpal, *Nano Lett.*, 2013, **14**, 101-106.

15. T. V. Shahbazyan, *Nano Lett.*, 2012, **13**, 194-198.
16. J. Yoo, X. Ma, W. Tang and G.-C. Yi, *Nano Lett.*, 2013, **13**, 2134-2140.
17. L. Zhao, T. Ming, L. Shao, H. Chen and J. Wang, *J. Phys. Chem. C*, 2012, **116**, 8287-8296.
18. M. Lunz, V. A. Gerard, Y. K. Gun'ko, V. Lesnyak, N. Gaponik, A. S. Susha, A. L. Rogach and A. L. Bradley, *Nano Lett.*, 2011, **11**, 3341-3345.
19. C.C. Chang, Y. D. Sharma, Y.S. Kim, J. A. Bur, R. V. Shenoi, S. Krishna, D. Huang and S.-Y. Lin, *Nano Lett.*, 2010, **10**, 1704-1709.
20. S. Jin, E. DeMarco, M. J. Pellin, O. K. Farha, G. P. Wiederrecht and J. T. Hupp, *J. Phys. Chem. Lett.*, 2013, **4**, 3527-3533.
21. M. J. Previte, K. Aslan, Y. Zhang and C. D. Geddes, *J. Phys Chem. C*, 2007, **111**, 6051-6059.
22. M. Banik, P. Z. El-Khoury, A. Nag, A. Rodriguez-Perez, N. Guarrottxena, G. C. Bazan and V. A. Apkarian, *ACS Nano*, 2012, **6**, 10343-10354.
23. L.-B. Zhao, M. Zhang, Y.-F. Huang, C. T. Williams, D.-Y. Wu, B. Ren and Z.-Q. Tian, *J. Phys. Chem. Lett.,* 2014, **5**, 1259-1266.
24. W. M. Leevy, S. T. Gammon, H. Jiang, J. R. Johnson, D. J. Maxwell, E. N. Jackson, M. Marquez, D. Piwnica-Worms and B. D. Smith, *J. Am. Chem. Soc.*, 2006, **128**, 16476-16477.
25. K. Aslan, J. R. Lakowicz and C. D. Geddes, *J. Phys. Chem. B*, 2005, **109**, 6247-6251.
26. K. Aslan, Z. Leonenko, J. R. Lakowicz and C. D. Geddes, *J. Phys. Chem. B*, 2005, **109**, 3157-3162.
27. J. Chen, Y. Jin, N. Fahruddin and J. X. Zhao, *Langmuir*, 2013, **29**, 1584-1591.
28. M. Ganguly, A. Pal, Y. Negishi and T. Pal, *Langmuir*, 2013, **29**, 2033-2043.
29. L. Shang and G. U. Nienhaus, *Biophys. Rev.*, 2012, **4**, 313-322.
30. Y. Wang, J. Chen and J. Irudayaraj, *Acs Nano*, 2011, **5**, 9718-9725.
31. H. Qian, M. Zhu, Z. Wu and R. Jin, *Acc. Chem. Res.*, 2012, **45**, 1470-1479.
32. J.M. Liu, J.T. Chen and X.P. Yan, *Anal. Chem.*, 2013, **85**, 3238-3245.
33. F. Wen, Y. Dong, L. Feng, S. Wang, S. Zhang and X. Zhang, *Anal. Chem.*, 2011, **83**, 1193-1196.
34. B. Paramanik and A. Patra, *J. Mater. Chem. C*, 2014, **2**, 3005-3012.
35. H. Dai, Y. Shi, Y. Wang, Y. Sun, J. Hu, P. Ni and Z. Li, *Biosens. Bioelectron.*, 2014, **53**, 76-81.
36. J.-a. Annie Ho, H.-C. Chang and W.-T. Su, *Ana. Chem.*, 2012, **84**, 3246-3253.
37. Y.-H. Lin and W.-L. Tseng, *Anal. Chem.*, 2010, **82**, 9194-9200.
38. D. Hu, Z. Sheng, P. Gong, P. Zhang and L. Cai, *Analyst*, 2010, **135**, 1411-1416.
39. M. Zhang and B.-C. Ye, *Analyst*, 2011, **136**, 5139-5142.
40. H. Liu, X. Zhang, X. Wu, L. Jiang, C. Burda and J.-J. Zhu, *Chem. Commun.*, 2011, **47**, 4237-4239.
41. M.-L. Cui, J.-M. Liu, X.-X. Wang, L.-P. Lin, L. Jiao, L.-H. Zhang, Z.-Y. Zheng and S.-Q. Lin, *Analyst*, 2012, **137**, 5346-5351.
42. V. Venkatesh, A. Shukla, S. Sivakumar and S. Verma, *ACS Appl. Mater. Inter.*, 2014, **6**, 2185-2191.
43. Z. Wu and R. Jin, *Nano Lett.*, 2010, **10**, 2568-2573.
44. J. Xie, Y. Zheng and J. Y. Ying, *J. Am. Chem. Soc.*, 2009, **131**, 888-889.
45. X. Zhang, C. A. Marocico, M. Lunz, V. A. Gerard, Y. K. Gun'ko, V. Lesnyak, N. Gaponik, A. S. Susha, A. L. Rogach and A. L. Bradley, *ACS Nano*, 2014, **8**, 1273-1283.
46. H. Aouani, J. Wenger, D. Gérard, H. Rigneault, E. Devaux, T. W. Ebbesen, F. Mahdavi, T. Xu and S. Blair, *ACS Nano*, 2009, **3**, 2043-2048.
47. R. Bardhan, N. K. Grady, J. R. Cole, A. Joshi and N. J. Halas, *ACS Nano*, 2009, **3**, 744-752.
48. S. Raut, R. Rich, R. Fudala, S. Butler, R. Kokate, Z. Gryczynski, R. Luchowski and I. Gryczynski, *Nanoscale*, 2014, **6**, 385-391.

49. D. S. Wilson and J. W. Szostak, *Ann. Rev. Biochem.*, 1999, **68**, 611-647.
50. J. Liu, Z. Cao and Y. Lu, *Chem. Rev.*, 2009, **109**, 1948-1998.
51. S. Song, L. Wang, J. Li, C. Fan and J. Zhao, *Trends Anal. Chem.*, 2008, **27**, 108-117.
52. D. Li, S. Song and C. Fan, *Acc. Chem. Res.*, 2010, **43**, 631-641.

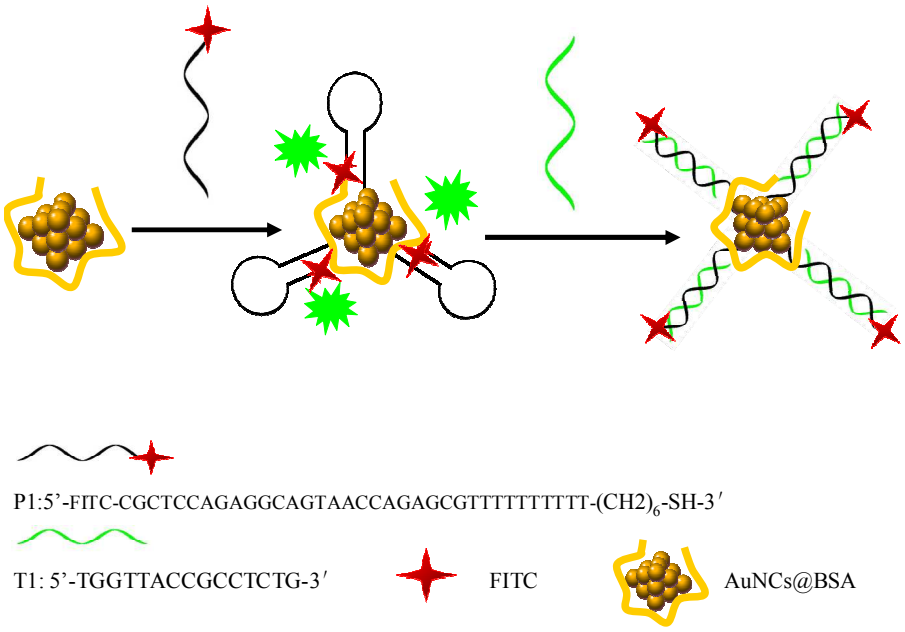

Scheme 1. The novel platform for detection of protooncogene based on Au nanoclusters

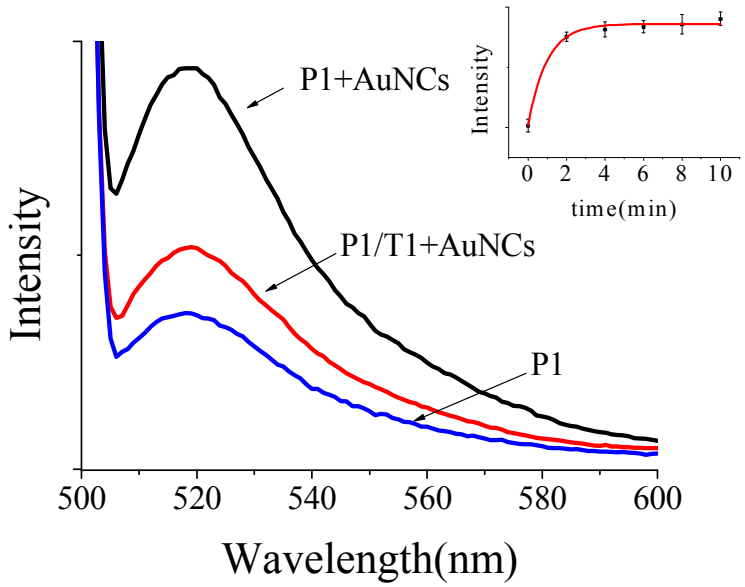

Figure 1. Fluorescence spectra of P1+AuNCs (10 nM P1 with AuNCs), P1/T1 duplex +AuNCs (10 nM P1 and 50 nM T1 with AuNCs) and P1 (10 nM P1 without AuNCs). Inset: Kinetic study for the fluorescence change of P1 in the presence of AuNCs. Excitation and emission wavelengths are 490 and 520 nm, respectively.

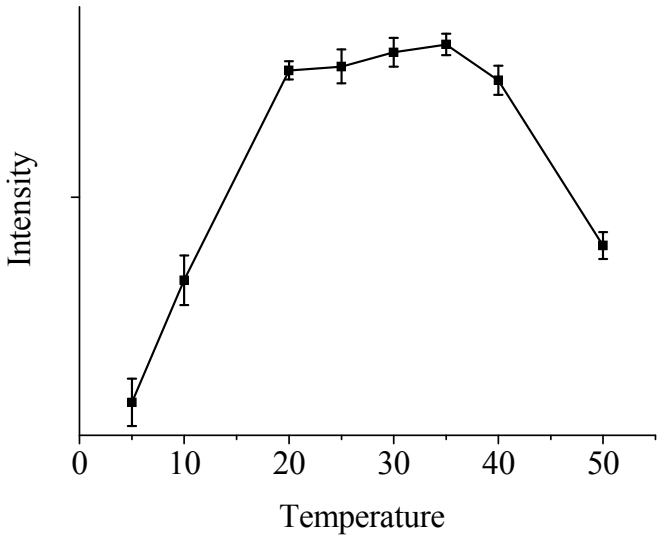

Figure 2. Temperature dependences of the FITC fluorescence intensity (enhanced fluorescence spectra of 10nM P1 in the presence of AuNCs at 5, 10, 20, 25, 30, 35, 40 and 50□).

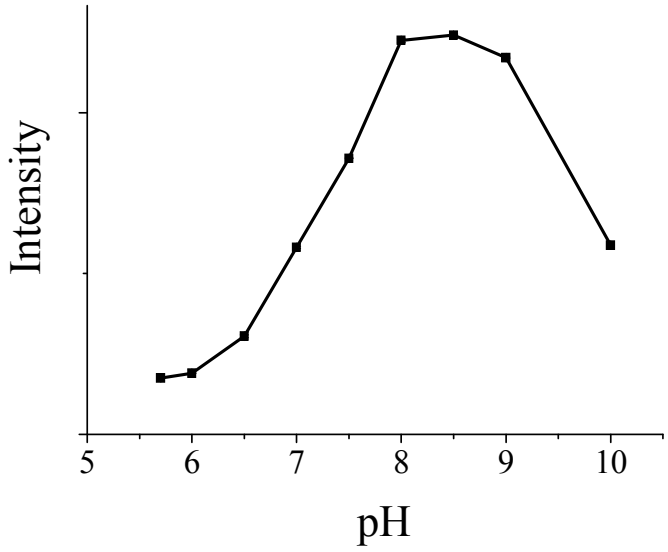

Figure 3. The pH (pH 5.5, 6.0, 7.0, 7.5, 8.0, 8.5, 9.0 and 10) dependences of the FITC fluorescence intensity (fluorescence spectra of 10 nM P1 in the presence of AuNCs)

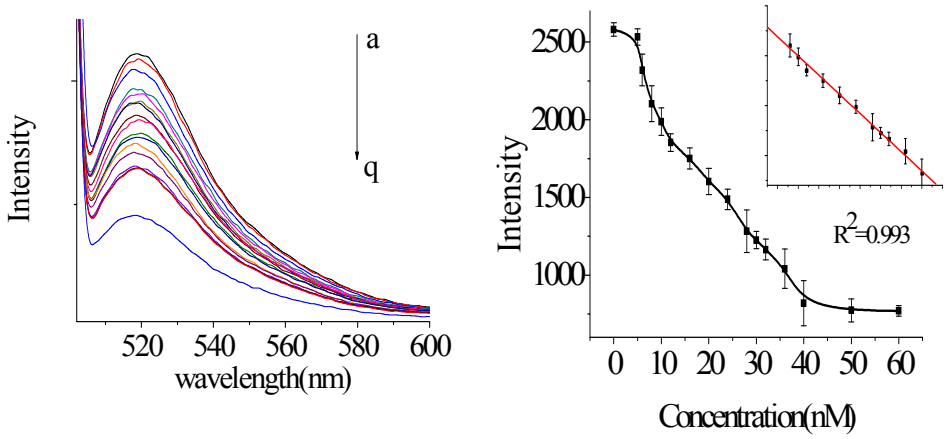

(a) (b)

Figure 4. (a) The calibration curve for DNA detection (a-p: 0, 5, 6, 8, 10, 12, 16, 20, 24, 28, 30, 32, 36, 40, 50 and 60 nM. q: 10 nM P1 in PBS buffer witnout AuNCs). (b) Fluorescence spectra of P1 (10 nM) with AuNCs in the presence of different concentrations of T1 (0, 5, 6, 8, 10, 12, 16, 20, 24, 28, 30, 32, 36, 40, 50 and 60 nM). Inset: amplification of the linear concentration range of the calibration curve. Excitation and emission wavelengths are 490 and 520 nm, respectively.

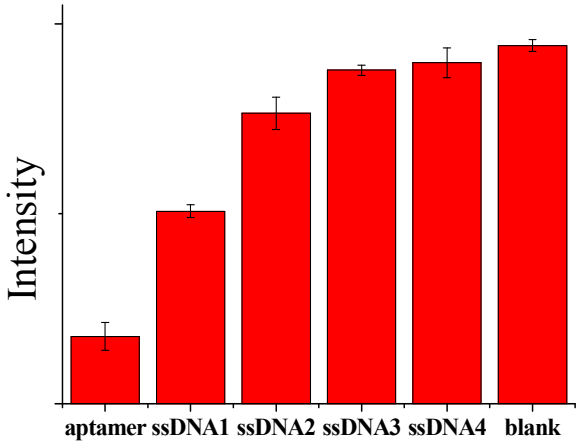

Figure 5. Selectivity of the AuNCs-based protooncogene sensor over ssDNA1, ssDN2, ssDNA3, ssDNA 4 and blank sample (each 10uM). Excitation and emission wavelengths are 490 and 520 nm, respectively.